

Adaptive step size selection for Hessian-based manifold Langevin samplers^{*}

Tore Selland Kleppe[†]

September 3, 2015

Abstract

The usage of positive definite metric tensors derived from second derivative information in the context of the simplified manifold Metropolis adjusted Langevin algorithm (MALA) is explored. A new adaptive step size procedure that resolves the shortcomings of such metric tensors in regions where the log-target has near zero curvature in some direction is proposed. The adaptive step size selection also appears to alleviate the need for different tuning parameters in transient and stationary regimes that is typical of MALA. The combination of metric tensors derived from second derivative information and adaptive step size selection constitute a large step towards developing reliable manifold MCMC methods that can be implemented automatically for models with unknown or intractable Fisher information, and even for target distributions that do not admit factorization into prior and likelihood. Through examples of low to moderate dimension, it is shown that proposed methodology performs very well relative to alternative MCMC methods.

Keywords: Adaptive step size, Hamiltonian Monte Carlo, Manifold Langevin, MCMC, Modified Cholesky algorithm

1 Introduction

Suppose $\tilde{\pi}(\mathbf{x})$ is a target density kernel where $\mathbf{x} \in \mathbb{R}^d$ so that $\pi(\mathbf{x}) = \tilde{\pi}(\mathbf{x}) / \int \tilde{\pi}(\mathbf{x}) d\mathbf{x}$ is a probability density function. Bayesian analysis of many statistical models necessitates the calculation of integrals with respect to $\pi(\mathbf{x})$ when $\pi(\mathbf{x})$ is analytically intractable and only the unnormalized density kernel $\tilde{\pi}(\mathbf{x})$ is available for evaluation (see e.g. Gelman et al., 2014). To approximate such integrals, Markov Chain Monte Carlo (MCMC)

^{*}The author is indebted to the reviewers, Hans A. Karlsen, Hans J. Skaug, Anders Tranberg and participants at the 18th meeting of the Norwegian Statistical Association for valuable comments.

[†]University of Stavanger, tore.kleppe@uis.no

has seen widespread use, and the development of better MCMC algorithms that can help researchers tackle even larger and more challenging models is still a highly active field (see e.g. Andrieu et al., 2010; Brooks et al., 2011; Girolami and Calderhead, 2011).

MCMC relies on constructing a discrete time Markov process $\{\mathbf{x}_t\}$ that has $\pi(\mathbf{x})$ as its stationary distribution. Consequently, an ergodic theorem ensures that, under some technical conditions, integrals on the form $\int g(\mathbf{x})\pi(\mathbf{x})d\mathbf{x}$ can be approximated as $\hat{\mu}_T(g) = \frac{1}{T} \sum_{t=1}^T g(\mathbf{x}_t)$ for some large T (e.g. Robert and Casella, 2004, chapter 6). A very general way of constructing such a Markov process, and that serves as the foundation of most MCMC methods, is the Metropolis Hastings (MH) algorithm (Metropolis et al., 1953; Hastings, 1970). Suppose the current state of the Markov process is \mathbf{x}_t and that $q(\cdot|\mathbf{x}_t)$ is some proposal probability density function. Then the MH algorithm proceeds by proposing $\mathbf{x}^* \sim q(\cdot|\mathbf{x}_t)$, and accepting the new state \mathbf{x}_{t+1} to be equal to \mathbf{x}^* with probability $\alpha(\mathbf{x}_t, \mathbf{x}^*) = \min[1, \tilde{\pi}(\mathbf{x}^*)q(\mathbf{x}_t|\mathbf{x}^*)/(\tilde{\pi}(\mathbf{x}_t)q(\mathbf{x}^*|\mathbf{x}_t))]$. With remaining probability $1 - \alpha(\mathbf{x}_t, \mathbf{x}^*)$, \mathbf{x}_{t+1} is set equal to \mathbf{x}_t . The MH algorithm is extremely general as only minimal restrictions on the proposal density are necessary for $\{\mathbf{x}_t\}$ to satisfy detailed balance with $\pi(\mathbf{x})$ as the stationary distribution (Robert and Casella, 2004).

These minimal restrictions have led to a large number of strategies for choosing proposal distributions (see e.g. Liu, 2001; Robert and Casella, 2004). The most widespread strategy is the Gaussian random walk proposal, corresponding to $q(\cdot|\mathbf{x}_t) = \mathcal{N}(\cdot|\mathbf{x}_t, \Sigma)$ where $\mathcal{N}(\mathbf{x}|\mu, \Sigma)$ denotes the $N(\mu, \Sigma)$ density evaluated at \mathbf{x} . The covariance matrix Σ should be chosen according to the target distribution at hand. As a rule of thumb, a scale of $q(\cdot|\mathbf{x}_t)$ that is “large” relative to the scale of the target density leads to a low acceptance probability, and thereby a slow exploration of target distribution. At the other end of the spectrum, if the scale of $q(\cdot|\mathbf{x}_t)$ is “small” relative to the scale of the target, one typically obtains a high acceptance probability but the cumulative distance traversed by many accepted steps will still be small. Provided that the variance of $\hat{\mu}_T(g)$ exists, both extreme cases lead to the variance of $\hat{\mu}_T(g)$ being large for fixed T , whereas intermediate choices of scale typically lead to more efficient sampling in the sense that the variance of $\hat{\mu}_T(g)$ is smaller for fixed T than the variance at the extreme cases. It should be noted that “large” and “small” scales relative to the target are not absolute or even well-defined magnitudes, and depend among many other aspects, on the dimension d of the target (see e.g. Gelman et al., 1996; Roberts and Rosenthal, 2001). An additional complication is that many target distributions of interest, e.g. joint posterior distributions of latent variables and variance parameter of the latent variables, contain significantly different scaling properties in different regions of the support of the target. Consequently, there is often a need for proposal distributions to adapt to local properties of the target distribution to achieve efficient sampling.

Many researchers have explored MCMC methods that exploit local derivative information from the target distribution to obtain more efficient sampling. Early contributions in this strand of the literature includes

the Metropolis adjusted Langevin algorithm (MALA) (see e.g. Roberts and Tweedie, 1996; Roberts and Stramer, 2002). MALA is a special case of the MH algorithm where the proposal distribution is equal to a time-discretization of a Langevin diffusion, where the Langevin diffusion has the target distribution as its stationary distribution. The drift term in such diffusion, and consequently the mean of the proposal distribution, will depend on the gradient of $\log \tilde{\pi}(\mathbf{x})$. To achieve reasonable acceptance rates, it is often necessary to choose the (time-) step size of the proposal distribution rather small, and it has been argued that the MALA in this case will revert to a behavior similar to that of the random walk MH (Neal, 2010).

Another way of constructing MCMC samplers that exploit derivative information is Hamiltonian (or Hybrid) Monte Carlo (HMC) (Duane et al., 1987; Liu, 2001; Neal, 2010; Beskos et al., 2013; Betancourt et al., 2014; Hoffman and Gelman, 2014). HMC has the potential of producing proposals that are far from the current state, while retaining arbitrarily high acceptance rates. The proposals originate from numerically integrating a set of ordinary differential equations that involve the gradient of $\log \tilde{\pi}(\mathbf{x})$ and it is often necessary to evaluate this gradient hundreds of times per proposed state to achieve reasonable acceptance rates while retaining proposals that are far from the current state.

Most implementations of MALA and HMC involve a user-specified scaling matrix (in addition to other tuning parameters) to achieve reasonable efficiency. In a landmark paper, Girolami and Calderhead (2011) proposes to recast MALA and HMC on a Riemann manifold that respects the local scaling properties of the target, and consequently alleviates the need to choose a global scaling matrix. Suppose \mathbf{x} are the parameters to be sampled and \mathbf{y} the observations associated with a Bayesian statistical model that admit the explicit factorization into data likelihood $p(\mathbf{y}|\mathbf{x})$ and prior distribution $p(\mathbf{x})$, i.e. $\tilde{\pi}(\mathbf{x}) \propto p(\mathbf{y}|\mathbf{x})p(\mathbf{x})$. Then Girolami and Calderhead (2011) took their metric tensor to be the matrix

$$G_{GC}(\mathbf{x}) = -E_{p(\mathbf{y}|\mathbf{x})} [\nabla_{\mathbf{x}}^2 \log p(\mathbf{y}|\mathbf{x})] - \nabla_{\mathbf{x}}^2 \log p(\mathbf{x}), \quad (1)$$

namely the Fisher information matrix associated with data likelihood plus the negative Hessian of the log-prior. This choice was demonstrated to be highly suited for Langevin and Hamiltonian based algorithms that take local scaling properties into account. However, due to the expectation in (1), the Fisher information matrix is rarely available in closed form, and the potential for automating the implementation of MCMC samplers based on such a metric seems a formidable task.

In this paper, an alternative approach based on deriving a metric tensor for simplified manifold MALA directly from the negative Hessian of $\log \tilde{\pi}(\mathbf{x})$ is explored. As noted by Girolami and Calderhead (2011) and several of the discussants of that paper (see e.g. Sanz-Serna, 2011; Guerrero et al., 2011; Jasra and Singh, 2011), this approach admit a high degree of automation via e.g. the usage of automatic differentiation software

(Griewank, 2000), but is complicated by the fact that the negative Hessian is typically not positive definite over the complete support of the target. Obtaining positive definite local scaling matrices from potentially indefinite Hessian matrices for application in modified Newton methods has seen substantial treatment in non-convex numerical optimization literature (see section 6.3 of Nocedal and Wright, 1999, for an overview). Such approaches typically rely on either modification of the eigenvalues via a full spectral decomposition of the Hessian, or some form of modified Cholesky algorithm that produces a factorization of a symmetric positive definite matrix that is close to the Hessian in some metric. In the MCMC context, the former approach was taken by Martin et al. (2012); Betancourt (2013), whereas in the present paper I advocate the latter as it has potential to exploit sparsity of the Hessian.

The added generality with respect to target densities that can be handled by Hessian-based metric tensors (based either on the spectral decomposition or modified Cholesky factorizations) relative to (1) comes at the cost of potential pathological behavior in regions of the log-target with near zero curvature in some direction. To counteract such effects, the primary contribution of this paper is a new adaptive step size procedure for simplified manifold MALA that chooses the step size locally based how well the Hessian-based metric tensor reflects the local scaling of the target. The adaptive step size procedure remains active throughout the MCMC simulation and at the same time retains the target as the stationary distribution. The adaptive step size procedure exploits the well known fact that a MALA update is equivalent to a particular HMC method using one time integration step (Neal, 2010), and therefore admits selection of step sizes for simplified manifold MALA based on the (dimensionless) energy error of the associated Hamiltonian system. An additional pro of the adaptive step size procedure is that it appears to alleviate the need for different tuning parameters in transient and stationary regimes that is typical for standard MALA implementations (Christensen et al., 2005).

The remaining of the paper is laid out as follows. Section 2 describes the applied metric tensor and the adaptive step size selection, and illustrates the proposed methodology using a pilot example. Section 3 illustrates the proposed methodology on two realistic example models, and compares the proposed methodology to alternative MCMC methods. Finally section 4 provides some discussion.

2 Adaptive step size modified Hessian MALA

Assume that $\tilde{\pi}(\mathbf{x})$ is sufficiently smooth to admit continuous and bounded derivatives up to order 2. I denote the gradient of the log-kernel $g(\mathbf{x}) = \nabla_{\mathbf{x}} \log \tilde{\pi}(\mathbf{x})$ and the Hessian of the log-kernel as $H(\mathbf{x}) = \nabla_{\mathbf{x}}^2 \log \tilde{\pi}(\mathbf{x})$. The $d \times d$ identity matrix is denoted I_d .

I take as vantage point the simplified manifold MALA (sMMALA) or position specific preconditioned

MALA of Girolami and Calderhead (2011) (see also Livingstone and Girolami, 2014; Xifara et al., 2014), which is a MH method characterized by the proposal distribution

$$q(\cdot|\mathbf{x}) = \mathcal{N}\left(\cdot|\mathbf{x} + \frac{\varepsilon^2}{2} [G(\mathbf{x})]^{-1} g(\mathbf{x}), \varepsilon^2 [G(\mathbf{x})]^{-1}\right). \quad (2)$$

Here $G(\mathbf{x})$ is a $d \times d$ symmetric and positive definite matrix, from now on referred to as the metric tensor, and ε is a tunable step size.

2.1 Modified Cholesky based metric tensor

This section explains a metric tensor based on an adaptation of the modified Cholesky decomposition of Gill and Murray (1974), Gill et al. (1981), from now on referred to as GMW. Suppose $A \in \mathbb{R}^{d \times d}$ is a symmetric, not necessarily positive definite matrix. Given a user-specified small positive scale parameter u , our adaptation of GMW (details and algorithm in Appendix A) aims at finding a Cholesky decomposition LL^T where L is lower triangular so that

$$\hat{A} = LL^T = A + J, \text{ where } L_{i,i}^2 \geq u \max\left(1, \max_{1 \leq i,j \leq d} |A_{i,j}|\right) > 0, \quad i = 1, \dots, d. \quad (3)$$

The matrix J is a diagonal matrix with non-negative elements chosen to ensure that \hat{A} is positive definite, and in particular the design of the GMW Cholesky algorithm ensures that if A is sufficiently positive definite, then $J = 0$. As J is a diagonal matrix and assuming that A has non-zero diagonal elements, the sparsity structures of A and $A + J$ are identical. This implies that whenever A has a sparsity structure that can be exploited using sparse numerical Cholesky factorizations (Davis, 2006), the same applies for the GMW factorization.

The GMW factorization has seen widespread use within the numerical optimization literature as a key ingredient in practical Newton optimization algorithms for non-convex optimization problems (Nocedal and Wright, 1999), and has also served as the basis for further refinements as in Schnabel and Eskow (1990, 1999). For simplicity, I employ a variant of the algorithm given in Gill et al. (1981).

In the remainder of this paper I work with the modified Hessian metric tensor

$$G_{MC}(\mathbf{x}) = L(\mathbf{x})L(\mathbf{x})^T,$$

where $L(\mathbf{x})$ is the output from the GMW Cholesky factorization (3) applied to $-H(\mathbf{x})$. In itself, this approach for finding a metric tensor is not fail-safe. To see this, consider for instance the $d = 1$ case, for which the

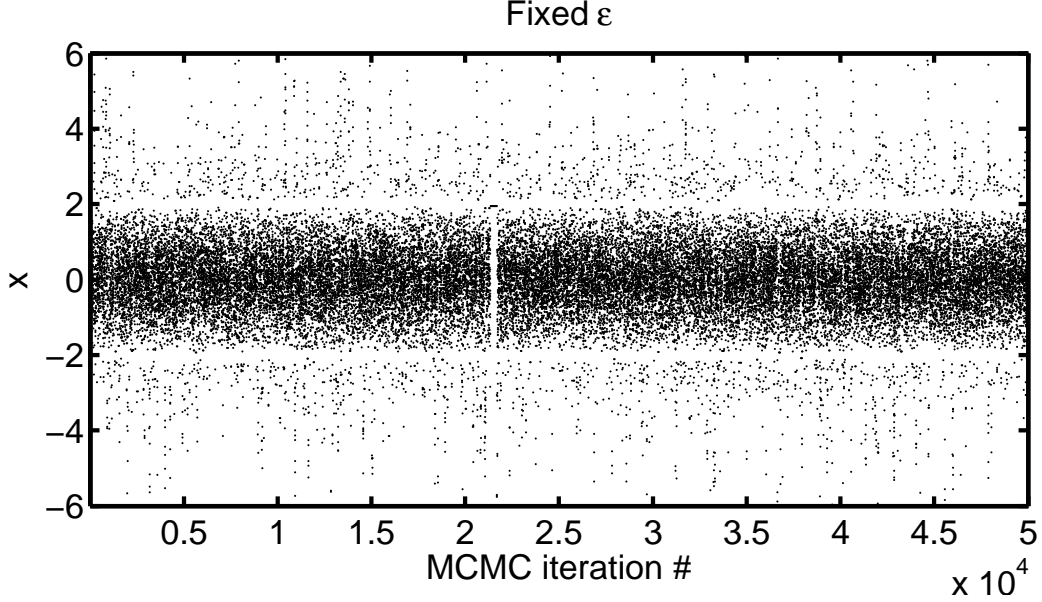


Figure 1: 50,000 iterations of sMMALA with metric tensor (4), $u = 0.001$ and $\varepsilon = 0.75$ applied to a t -distribution with 4 degrees of freedom. It is seen that the chain rarely enters the regions near $|\mathbf{x}|=2$, and when it does, it tends to get stuck. An example of this is seen starting in iteration 21347 where the chain is stuck for 340 iterations at approximately 1.9529.

proposed metric tensor reduces to

$$G_{MC}(\mathbf{x}) = \max(u, |H(\mathbf{x})|). \quad (4)$$

Typically I take u to be rather small in order not to disturb the proposal mechanism of sMMALA (2) in regions where $|H(\mathbf{x})|$ is small but still contains useful information on the local scaling properties of the target distribution. However if left unmodified, a sMMALA method based on (4) would very infrequently move into regions near roots of the second derivative (inflection points). To see this, observe that the backward transition density $q(\mathbf{x}_t|\mathbf{x}^*)$ occurring in the nominator of the acceptance probability will be

$$q(\mathbf{x}_t|\mathbf{x}^*) = O(\sqrt{u}/\varepsilon) \text{ when } G(\mathbf{x}^*) = u. \quad (5)$$

When the method has moved into such a region, the chain will tend to be stuck for many iterations as the proposal distribution then has too large variance.

To illustrate this phenomenon, consider a t -distributed target with 4 degrees of freedom. In this case there are two inflection points of the log-density located at $|\mathbf{x}| = 2$. Figure 1 shows 50,000 MCMC iterations using sMMALA based on (4) for this target. It is seen that the chain rarely enters the regions close to the inflection points, and when it does, the chain tend to get stuck. It is worth noticing that these effects are not unique to the modified Cholesky approach. Specifically, (4) would also be the result if the metric tensor was

computed by modifying the eigenvalues of a full spectral decomposition as in Martin et al. (2012), and the metric tensor would be a soft/regularized absolute value applied to $H(\mathbf{x})$ in the methodology of Betancourt (2013). Rather the effects are the cost of the added generality associated with using second order derivative information directly rather than via the Fisher information matrix as in Girolami and Calderhead (2011). To mitigate these undesirable effects, (5) suggest either that u or ε must be chosen adaptively. In this work, I focus on the latter as a simple and computationally efficient method can be implemented for this purpose.

2.2 sMMALA with randomized adaptive selection of ε

In this work, I propose to select the proposal step size as a function of the current state \mathbf{x}_t and an easily simulated auxiliary random variable $\mathbf{w}_t \sim \pi(\mathbf{w})$, namely $\varepsilon = \varepsilon(\mathbf{x}_t, \mathbf{w}_t)$. The role of \mathbf{w} is essentially to randomize the step size, and a further motivation for including it will be clear from section 2.3 when the functional forms of $\varepsilon(\cdot, \cdot)$ advocated here are discussed. Before that, I introduce the an overarching sampling algorithm in the form of a Metropolis within Gibbs sampler based on the sMMALA update where invariant distribution will be shown to be the augmented target

$$\pi(\mathbf{x}, \mathbf{w}) = \pi(\mathbf{x})\pi(\mathbf{w}). \quad (6)$$

Notice that the algorithm with target (6) is primarily a construct to make the method time-homogenous and thereby enabling easy establishment of convergence results when an adaptive step size selection $\varepsilon(\mathbf{x}, \mathbf{w})$ is employed. In practice only the \mathbf{x} -subchain is of interest.

Given the current configuration $(\mathbf{x}_t, \mathbf{w}_t) \sim \pi(\mathbf{x}, \mathbf{w})$, one step of the proposed Metropolis within Gibbs sampler (see e.g. Robert and Casella, 2004, Algorithm A.43) based on sMMALA for the augmented target may then be summarized by the steps

1. Compute forward step size $\varepsilon_f = \varepsilon(\mathbf{x}_t, \mathbf{w}_t)$.
2. Draw proposal $\mathbf{x}_{t+1}^* \sim N(\mathbf{x}_t + \frac{\varepsilon_f^2}{2} G^{-1}(\mathbf{x}_t)g(\mathbf{x}_t), \varepsilon_f^2 G^{-1}(\mathbf{x}_t))$.
3. Compute backward step size $\varepsilon_b = \varepsilon(\mathbf{x}_{t+1}^*, \mathbf{w}_t)$.
4. Compute MH accept probability

$$\alpha(\mathbf{x}_t, \mathbf{x}_{t+1}^*) = \min \left(1, \frac{\tilde{\pi}(\mathbf{x}_{t+1}^*) \mathcal{N} \left(\mathbf{x}_t | \mathbf{x}_{t+1}^* + \frac{\varepsilon_b^2}{2} G^{-1}(\mathbf{x}_{t+1}^*)g(\mathbf{x}_{t+1}^*), \varepsilon_b^2 G^{-1}(\mathbf{x}_{t+1}^*) \right)}{\tilde{\pi}(\mathbf{x}_t) \mathcal{N} \left(\mathbf{x}_{t+1}^* | \mathbf{x}_t + \frac{\varepsilon_f^2}{2} G^{-1}(\mathbf{x}_t)g(\mathbf{x}_t), \varepsilon_f^2 G^{-1}(\mathbf{x}_t) \right)} \right).$$

Let $\mathbf{x}_{t+1} = \mathbf{x}_{t+1}^*$ with probability $\alpha(\mathbf{x}_t, \mathbf{x}_{t+1}^*)$ and let $\mathbf{x}_{t+1} = \mathbf{x}_t$ with remaining probability.

5. Draw $\mathbf{w}_{t+1} \sim \pi(\mathbf{w})$.

Notice in particular that $\varepsilon_f, \varepsilon_b$ are computed using the same \mathbf{w} -argument and therefore steps 1-4 constitute a reversible MH step for each \mathbf{w} . Based on this observation, I prove following result:

Proposition 1: *Provided that $0 < \varepsilon(\mathbf{x}, \mathbf{w}) < \infty$ for each (\mathbf{x}, \mathbf{w}) in the support of $\pi(\mathbf{x}, \mathbf{w})$, the Metropolis within Gibbs sampler in steps 1-5 is $\pi(\mathbf{x}, \mathbf{w})$ -irreducible, aperiodic and has $\pi(\mathbf{x}, \mathbf{w})$ as invariant distribution.*

The proof is given in Appendix B and relies on the fact that for a Metropolis within Gibbs sampler, the parameters of the proposal distribution in the MH step for updating one block (\mathbf{x}) may depend on the current state of the remaining blocks (\mathbf{w}) (see e.g. Gilks et al., 1994; Robert and Casella, 2004; Zhang and Sutton, 2011). Note in particular that steps 1-5 do not fulfill detailed balance for target $\pi(\mathbf{x}, \mathbf{w})$. On the other hand, a (time-inhomogenous due to changing \mathbf{w}) detailed balance holds for each transition of the \mathbf{x} -subchain. Having established that such adaptive selection of step size does not disturb the invariant distribution of the \mathbf{x} -subchain for a large class of functions $\varepsilon(\cdot, \cdot)$, I now consider the specific functional forms of $\varepsilon(\cdot, \cdot)$ I advocate.

2.3 Adaptive step size selection based on Hamiltonian dynamics

The method for selection of ε uses a well-known duality between MALA and HMC, namely that the proposal of MALA corresponds to a single time-integration step of Euclidian metric HMC starting at \mathbf{x}_t when the leap frog integrator (Leimkuhler and Reich, 2004) is employed (Neal, 2010). Here I propose to choose the step size for sMMALA so that the energy error of a single trial step of the corresponding (Euclidian metric) HMC method with mass matrix $G(\mathbf{x}_t)$ is below a tunable threshold. The rationale for such an approach is that the absolute energy error provides a measure of time integration error that is comparable across different areas of the target density, and that will be large if the local scaling properties of $\log \pi(\mathbf{x})$ are poorly reflected by $G(\mathbf{x})$, as in the student t -pilot example discussed above. Computing the absolute energy error of the trial step is inexpensive relative to e.g. doing complete trial sMMALA steps for different values of ε , with the computational cost typically dominated by a few additional gradient evaluations.

To implement such energy error based selection $\varepsilon(\cdot, \cdot)$, I first take $\pi(\mathbf{w})$ to be a d -dimensional standard Gaussian variable. Given the current configuration of $(\mathbf{x}_t, \mathbf{w}_t)$, I define the position specific dummy Hamiltonian

$$\mathcal{H}(\mathbf{q}(\tau), \mathbf{p}(\tau) | \mathbf{x}_t) = -\log \tilde{\pi}(\mathbf{q}(\tau)) + \frac{1}{2} \mathbf{p}(\tau)^T G(\mathbf{x}_t)^{-1} \mathbf{p}(\tau), \quad (7)$$

where $\mathbf{q}(\tau)$ denotes position and $\mathbf{p}(\tau)$ denotes momentum at fictional time τ . Then a single leap frog step of

(time-) size ε starting from $\mathbf{q}(0) = \mathbf{x}_t$ and $\mathbf{p}(0) = L(\mathbf{x}_t)\mathbf{w}_t$ is performed:

$$\begin{aligned} \mathbf{p}(\varepsilon/2) &= \mathbf{p}(0) + \frac{\varepsilon}{2}g(\mathbf{q}(0)) = L(\mathbf{x}_t)\mathbf{w}_t + \frac{\varepsilon}{2}g(\mathbf{x}_t), \\ \mathbf{q}(\varepsilon) &= \mathbf{q}(0) + \varepsilon G(\mathbf{x}_t)^{-1}\mathbf{p}(\varepsilon/2) = \mathbf{x}_t + \frac{\varepsilon^2}{2}G^{-1}(\mathbf{x}_t)g(\mathbf{x}_t) + \varepsilon L(\mathbf{x}_t)^{-T}\mathbf{w}_t = \mathbf{x}^*(\varepsilon|\mathbf{x}_t, \mathbf{w}_t), \\ \mathbf{p}(\varepsilon) &= \mathbf{p}(\varepsilon/2) + \frac{\varepsilon}{2}g(\mathbf{q}(\varepsilon)) = L(\mathbf{x}_t)\mathbf{w}_t + \frac{\varepsilon}{2}(g(\mathbf{x}_t) + g(\mathbf{x}^*(\varepsilon|\mathbf{x}_t, \mathbf{w}_t))). \end{aligned} \quad (8)$$

The trial proposal $\mathbf{x}^*(\varepsilon|\mathbf{x}_t, \mathbf{w}_t)$ would occur if the standard normal vector \mathbf{w}_t was used to generate a proposal from (2) with current state equal to \mathbf{x}_t and time step size ε . The energy error associated with this trial time integration step is given as

$$\begin{aligned} \Delta(\varepsilon|\mathbf{x}_t, \mathbf{w}_t) &= \mathcal{H}(\mathbf{q}(0), \mathbf{p}(0)|\mathbf{x}_t) - \mathcal{H}(\mathbf{q}(\varepsilon), \mathbf{p}(\varepsilon)|\mathbf{x}_t) \\ &= -\log \tilde{\pi}(\mathbf{x}_t) + \log \tilde{\pi}(\mathbf{x}^*(\varepsilon|\mathbf{x}_t, \mathbf{w}_t)) \\ &\quad - \frac{\varepsilon}{2}\mathbf{w}_t^T \mathbf{r} - \frac{\varepsilon^2}{8}\mathbf{r}^T \mathbf{r} \end{aligned}$$

where $\mathbf{r} = L(\mathbf{x}_t)^{-1}(g(\mathbf{x}_t) + g(\mathbf{x}^*(\varepsilon|\mathbf{x}_t, \mathbf{w}_t)))$. Based on the expression for $\Delta(\varepsilon|\mathbf{x}_t, \mathbf{w}_t)$, a possible method for choosing $\varepsilon = \varepsilon(\mathbf{x}, \mathbf{w})$ would involve the following steps:

Suppose $\gamma > 0$ is the tunable maximal allowable trial energy error, with lower values of γ corresponding to higher acceptance rates and smaller ε . Let $0 < \bar{\varepsilon} < \infty$ be the maximal step size and let ε_0 denote the smallest positive root in ε of $|\Delta(\varepsilon|\mathbf{x}, \mathbf{w})| = \gamma$. An idealized candidate for choosing ε is then $\varepsilon(\mathbf{x}, \mathbf{w}) = \min(\bar{\varepsilon}, \varepsilon_0)$. The $\varepsilon > 0$ bound required in Proposition 1 is automatically fulfilled as consequence smoothness assumptions on $\log \tilde{\pi}(\mathbf{x})$, and thus such a step size function would lead the sampling algorithm outlined in section 2.2 to have the correct invariant distribution. In practice, locating ε_0 would amount to solving an equation that involves the gradient of the log-target numerically, and for computational effectivity reasons I therefore propose a method for only approximating ε_0 in Section 2.4.

It is worth noticing that the Hamiltonian (7) should be interpreted in the Euclidian metric sense as a tool to measure the time integration error around $\mathbf{q}(0) = \mathbf{x}_t$, $\mathbf{p}(0) = L(\mathbf{x}_t)\mathbf{w}_t$ when $G(\mathbf{x}_t)$ is the fixed mass matrix. This is relevant for sMMALA as the distribution of proposed $\mathbf{q}(\varepsilon)$ -states is (2) in this case. Moreover, it is in contrast to interpreting (7) in a Riemann manifold HMC sense with Hamiltonian say $-\log \tilde{\pi}(\mathbf{q}) + \frac{1}{2}\mathbf{p}^T G(\mathbf{q})^{-1}\mathbf{p}$ (which is off target due to a missing $\frac{1}{2}\log |G(\mathbf{q})|$ term (Girolami and Calderhead, 2011; Betancourt, 2013)). Under the latter interpretation, the energy error is irrelevant for sMMALA as the proposed $\mathbf{q}(\varepsilon)$ will not be distributed according to (2) regardless of the numerical integrator being employed, as the time evolution of \mathbf{p} will involve the gradient of $\frac{1}{2}\mathbf{p}^T G(\mathbf{q})^{-1}\mathbf{p}$ with respect to \mathbf{q} . In the same vein, I notice that $\min(1, \exp(\Delta))$ cannot be interpreted as a trial acceptance probability for the sMMALA as

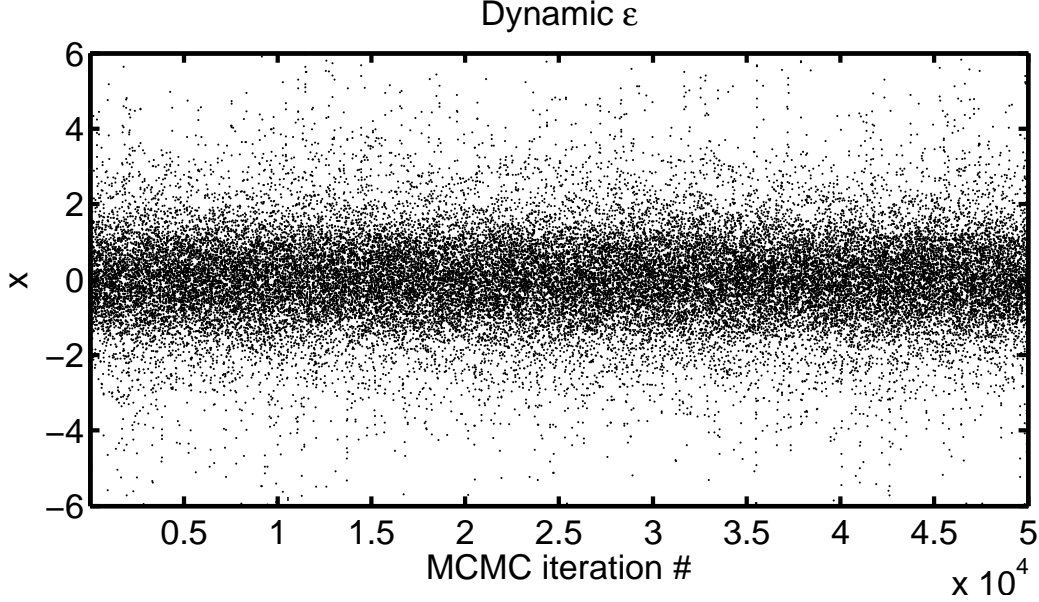


Figure 2: 50,000 iterations of sMMALA with metric tensor (4), $u = 0.001$, $\varepsilon(\mathbf{x}, \mathbf{w}) = \min(1, \varepsilon_0)$ as defined in the text and $\gamma = 1.0$ applied to a t -distribution with 4 degrees of freedom. It is seen that the adaptive selection of step size resolves sampling in the problematic regions around the inflection points.

the sMMALA deviates from being a reversible and volume-preserving discretization of either Hamiltonian when the \mathbf{x}_t -dependence of the mass matrix is taken into account in (7). Rather, γ should be interpreted as a tolerance of local (irreversible) time integration energy error, and in particular its relationship to the acceptance probability of the overall (reversible) sMMALA step is non-linear.

The role of \mathbf{w} is to act as typical (standardized) momentum variable that changes in each iteration of the overarching MCMC procedure to reflect the variation in the distribution of the proposal (2). A further potential candidate would be to integrate out \mathbf{w} , e.g. $\varepsilon(\mathbf{x}) = \int \varepsilon(\mathbf{x}, \mathbf{w}) \pi(\mathbf{w}) d\mathbf{w}$ so that steps 1-4 of section 2.2 would constitute a time-homogenous and reversible MH step. However even for moderate dimension d this becomes computationally intractable, as this integral has to be computed numerically. Further, it is not obvious that a deterministic (conditional on \mathbf{x}) step size $\varepsilon(\mathbf{x})$ has clear advantages over a stochastic step size $\varepsilon(\mathbf{x}, \mathbf{w})$.

To illustrate how the adaptive step size selection $\varepsilon(\mathbf{x}, \mathbf{w}) = \min(1, \varepsilon_0)$ resolves the shortcomings of sMMALA near inflection points, I consider again the t_4 -distribution target considered in section 2.1 with metric tensor (4). Figure 2 presents 50,000 MCMC iterations using adaptive step size sMMALA using a maximal absolute energy error $\gamma = 1.0$. It is seen that the adaptive step size selection resolves the inefficient sampling near the inflection points seen for the fixed step size implementation in Figure 1. Figure 3 shows the actual values of the (forward) adaptive step sizes $\varepsilon(\mathbf{x}_t, \mathbf{w}_t)$ as a function of \mathbf{x}_t , along with their expected value found by integrating out \mathbf{w} . It is seen that the energy error criterion appear to discriminate very well that the

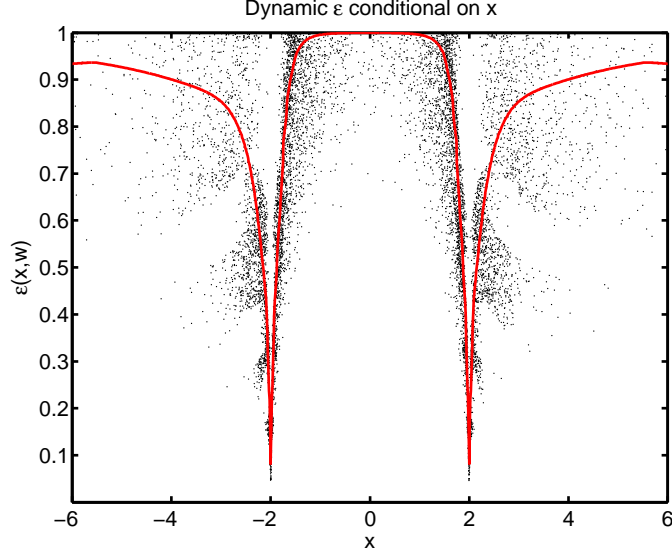


Figure 3: Values of the (forward) step size $\varepsilon(\mathbf{x}_t, \mathbf{w}_t) = \min(1, \varepsilon_0)$ as a function of \mathbf{x}_t for the simulation presented in Figure 2 are given as dots. The solid line indicates the average adaptive step size calculated as $\int \varepsilon(\mathbf{x}, \mathbf{w}) p(\mathbf{w}) d\mathbf{w}$ as a function of \mathbf{x} .

metric tensor (4) shows pathological behavior around the inflection points at $|\mathbf{x}| = 2$.

As pointed out by a reviewer, the above energy error argument can also be applied in non-adaptive step size sMMALA methods to locate regions of the support where deficiencies in the metric tensor lead to inefficient sampling analogous to what is seen in Figure 1. This is in particular of interest for $d \geq 3$, as then regions with inefficient sampling could be difficult to spot using e.g. trace or scatter plots. In practice, using energy error for such an end would amount to calculating the energy error associated with each proposed state. Specifically, suppose \mathbf{x}_t is the current state of a non-adaptive sMMALA method and $\mathbf{z} \sim N(0, I_d)$ is the standardized variable used to generate a proposal \mathbf{x}^* according to (2). The forward (backward) energy error Δ_t^f (Δ_t^b) associated with the proposal \mathbf{x}^* are given by

$$\begin{aligned} \Delta_t^f &= -\log \tilde{\pi}(\mathbf{x}_t) + \log \tilde{\pi}(\mathbf{x}^*) - \frac{\varepsilon}{2} \mathbf{z}^T \mathbf{r}_f - \frac{\varepsilon^2}{8} \mathbf{r}_f^T \mathbf{r}_f \\ \Delta_t^b &= -\log \tilde{\pi}(\mathbf{x}^*) + \log \tilde{\pi}(\mathbf{x}_t) - \frac{\varepsilon}{2} \mathbf{s}^T \mathbf{r}_b - \frac{\varepsilon^2}{8} \mathbf{r}_b^T \mathbf{r}_b \\ \mathbf{s} &= \varepsilon^{-1} L(\mathbf{x}^*)^T \left[\mathbf{x}_t - \mathbf{x}^* - \frac{\varepsilon^2}{2} G^{-1}(\mathbf{x}^*) g(\mathbf{x}^*) \right] \end{aligned}$$

where $\mathbf{r}_f = L(\mathbf{x}_t)^{-1} (g(\mathbf{x}_t) + g(\mathbf{x}^*))$ and $\mathbf{r}_b = L(\mathbf{x}^*)^{-1} (g(\mathbf{x}_t) + g(\mathbf{x}^*))$. A large $|\Delta_t^f|$ ($|\Delta_t^b|$) (e.g. $|\Delta_t^k| > 5$, $k = f, b$) will indicate that local scaling properties in the region around \mathbf{x}_t (\mathbf{x}^*) are poorly reflected by $G(\mathbf{x}_t)$ ($G(\mathbf{x}^*)$) and the user should consider revising the specification of G or at least reduce ε . Note in particular that Δ_t^k , $k = f, b$ can be computed in each iteration with minimal additional cost as the involved log-kernels, gradients and metric tensors must be computed anyway to form the acceptance probability for

Algorithm 1 Practical backtracking line search algorithm.

```
1: Set  $\varepsilon_1 \leftarrow 1$  (or some reasonable  $\bar{\varepsilon}$ )
2: Set  $\beta \leftarrow 10$  (or some reasonable energy error threshold).
3: Set  $\rho \leftarrow 0.5$  (or some reasonable step size decrement).
4: for ( $s = 1, 2, \dots$ )
5:   Compute  $|\Delta(\varepsilon_s | \mathbf{x}, \mathbf{w})|$ .
6:   if ( $|\Delta(\varepsilon_s | \mathbf{x}, \mathbf{w})| > \beta$ )
7:      $\varepsilon_{s+1} \leftarrow \rho \varepsilon_s$ .
8:   else
9:     if ( $|\Delta(\varepsilon_s | \mathbf{x}, \mathbf{w})| < \gamma$ )
10:      Return  $\varepsilon(\mathbf{x}, \mathbf{w}) = \varepsilon_s$ .
11:    else
12:       $\varepsilon_{s+1} \leftarrow 0.95 \left( \frac{\gamma}{|\Delta(\varepsilon_s | \mathbf{x}, \mathbf{w})|} \right)^{1/3} \varepsilon_s$ .
13:    end if
14:  end if
15: end for
```

proposal \mathbf{x}^* .

2.4 Practical implementation and choosing γ

For practical applications it is not necessary, nor desirable from a computational perspective, to find ε_0 with high precision. Rather a backtracking iterative scheme as exemplified in Algorithm 1 can be used. This algorithm is inspired by line searches commonly used numerical optimization (Nocedal and Wright, 1999) and the overarching idea is to generate a sequence trial step sizes $\bar{\varepsilon} = \varepsilon_1 > \varepsilon_2 > \dots$ until the criterion $|\Delta(\varepsilon_s | \mathbf{x}, \mathbf{w})| < \gamma$ is fulfilled. Algorithm 1 has two types of decrements, where in the case that absolute energy error is greater than β , the next trial step size is a factor $\rho < 1$ times the incumbent one. If the absolute energy error is smaller than β , but greater than γ , the choice of the next trial step size is informed by the fact that $\Delta(\varepsilon | \mathbf{x}, \mathbf{w}) = O(\varepsilon^3)$ for small ε . More specifically, I let next trial step ε_{s+1} be 0.95 times the root in ε of $\hat{\Delta}_s(\varepsilon) - \gamma$ where $\hat{\Delta}_s(\varepsilon) = (\varepsilon/\varepsilon_s)^3 |\Delta(\varepsilon_s | \mathbf{x}, \mathbf{w})|$ is the third order monomial that interpolates the observed absolute energy error at ε_s . The factor 0.95 is included to counteract slow convergence infrequently seen when $|\Delta(\varepsilon_s | \mathbf{x}, \mathbf{w})|$ is close to γ . Of course Algorithm 1 constitute only an example of how to implement $\varepsilon(\mathbf{x}, \mathbf{w})$, and may be further tuned and refined for each model instance without disturbing the stationary distribution as long as it remains the same throughout the MCMC simulation and fulfills the assumptions in Proposition 1. The cost of each iteration will typically be dominated by the gradient evaluation needed for computing \mathbf{r} for each trial ε .

For non-Gaussian targets, γ needs to be tuned to obtain e.g. the desired acceptance rate or to maximize

some more direct performance measure such as the expected jumping distance or effective sample size. The tuning could be done by e.g. dual averaging during the burn in iterations as in Hoffman and Gelman (2014). However, I have found that as a rule of thumb, values of γ between 1 and 2 tends to produce acceptable results for low to moderate-dimensional problems as the ones considered below. In this case, the adaptive step size selection typically produces long step sizes ($\varepsilon \sim \bar{\varepsilon}$) when G contains useful scaling information, but acts as safeguard and reduces the step size substantially when G shows some form of pathological behavior.

It is interesting to consider the impact of dimension d on the proposed adaptive step size selection, and consequently on the overall performance of the proposed methodology. For this purpose, I consider any d -dimensional non-degenerate $N(\mu, \Sigma)$ target, as it is rather straightforward to show that

$$E_{(\mathbf{x}, \mathbf{w})}(\Delta(\varepsilon|\mathbf{x}, \mathbf{w})) = d \left(\frac{1}{4} \varepsilon^4 - \frac{1}{32} \varepsilon^6 \right),$$

when $G(\mathbf{x}) = -H(\mathbf{x}) = \Sigma^{-1}$. For any fixed γ , which in the Gaussian case translates to a fixed acceptance rate invariant of d , the adaptive step size has leading term behavior $\varepsilon = O(d^{-1/4})$. Thus for high-dimensional target distributions, it is inevitable that adaptive step size sMMALA will revert to random walk behavior, and as a consequence I consider primarily low to moderate-dimensional applications as the primary scope.

3 Illustrations

This section considers example models and compares the proposed Adaptive step size Modified Hessian MALA (AMH-MALA) methodology to alternatives. The GARCH(1,1) model with t -distributed innovations considered first is included to highlight the behavior of AMH-MALA for a posterior distribution that exhibit strong non-linear dependence structures and has indefinite Hessian in substantial parts of the relevant parameter space. The Bayesian binary response regressions considered afterwards are included to allow for easy comparison with the methodology presented in Girolami and Calderhead (2011).

To compare the performance of different MCMC methods, I follow Girolami and Calderhead (2011) in estimating effective sample size (ESS) via the initial monotone sequence estimator of Geyer (1992), and in particular compare the minimum ESS (across the d dimensions of π) per second CPU-time spent obtaining the samples. All computations were carried out on a 2014 macbook pro with a 2 GHz Intel Core i7 processor and 8 GB of memory. The code used for the simulations is available at http://www.ux.uis.no/~tore/code/adaptive_langevin/, including a C++ function implementing the dense modified Cholesky factorization that can be called from Matlab.

| Method | CPU time (s) | α_0 ESS | α_1 ESS | β ESS | ν ESS | minimum ESS per second |
|---------------|-----------------|-------------------|-------------------|----------------|--------------|---------------------------|
| bayesGARCH | 18.7 | 80.0 | 52.9 | 48.2 | 63.9 | (2.46) |
| AMH-MALA | 140 | 283 | 310 | 252 | 398 | 1.79 |
| AMH-MALA(eig) | 146 | 251 | 262 | 229 | 424 | 1.51 |
| HMC | 2653 | 4738 | 2284 | 2503 | 4993 | 0.86 |

Table 1: Effective samples sizes and minimum effective samples sizes per second CPU time for different MCMC algorithms applied to the GARCH(1,1) model with t -distributed innovations. Best performances are indicated in bold font. All figures are calculated over 5000 MCMC iterations after burn in. Note that the bayesGARCH Gibbs sampler is partially written in C, and thus the CPU-time and minimum ESS per CPU time are not directly comparable to the remaining figures.

3.1 GARCH(1,1) model with t -distributed innovations

As the first realistic illustration I consider sampling the posterior parameters of a GARCH(1,1) model with t -distributed innovations (see e.g. McNeil et al., 2005, Chapter 4) for log-return observations y_1, \dots, y_T on the form

$$y_i = \sqrt{h_i} \eta_i, \eta_i = \sqrt{\frac{\nu-2}{\nu}} \tilde{\eta}_i, \tilde{\eta}_i \sim \text{iid } t(\nu), i = 1, \dots, T, \quad (9)$$

$$h_i = \alpha_0 + \alpha_1 y_{i-1}^2 + \beta h_{i-1}, i = 2, \dots, T, h_1 = \alpha_0. \quad (10)$$

The priors are taken from Ardia and Hoogerheide (2010) and are the default priors used in the associated **bayesGARCH** R-package for the same model. Specifically, $\alpha_0, \alpha_1, \beta$ have independent truncated normal priors $p(\alpha_k) \propto \exp(-\frac{1}{2} \frac{\alpha_k^2}{1000}) \mathbf{1}_{\{\alpha_k > 0\}}$, $k = 0, 1$ and $p(\beta) \propto \exp(-\frac{1}{2} \frac{\beta^2}{1000}) \mathbf{1}_{\{\beta > 0\}}$. The prior for the degrees of freedom parameter ν is a truncated exponential, namely $p(\nu) \propto \exp(-\nu/100) \mathbf{1}_{\{\nu > 2\}}$. For our illustration, I employ a data set of Deutschmark vs British Pound (DEM/GBP) foreign exchange rate log-returns at daily frequency, which is also included in the **bayesGARCH** package. The sample covers January 3, 1985 to December 31, 1991, and constitute $T = 1974$ log-return observations.

The proposed AMH-MALA methodology is compared to the Gibbs sampler implemented in the **bayesGARCH** package (Ardia and Hoogerheide, 2010) and HMC with mass matrix fixed to the identity matrix. For HMC I follow Girolami and Calderhead (2011) and choose 100 time integration steps and the integration step size was taken to be $\varepsilon = 0.0075 \pm 10\%$ uniform noise to attain acceptance rates of around 80%. In addition I also consider AMH-MALA implemented with a metric tensor similar to the one proposed by Betancourt (2013) and denote this by AMH-MALA(eig). Specifically, let λ_i denote the i th eigenvalue of $-H$. Then G has the same eigenvectors as $-H$ but the i th eigenvalue is taken as $\max(|\lambda_i|, 0.001)$. For both AMH-MALA methods, I use $\gamma = 1.0$ and Algorithm 1 with $\beta = 10.0$, $\rho = 0.5$ for adaptive step size selection. For AMH-MALA based on the modified Cholesky, I use $u = 0.001$. HMC and the AMH-MALA methods are applied in

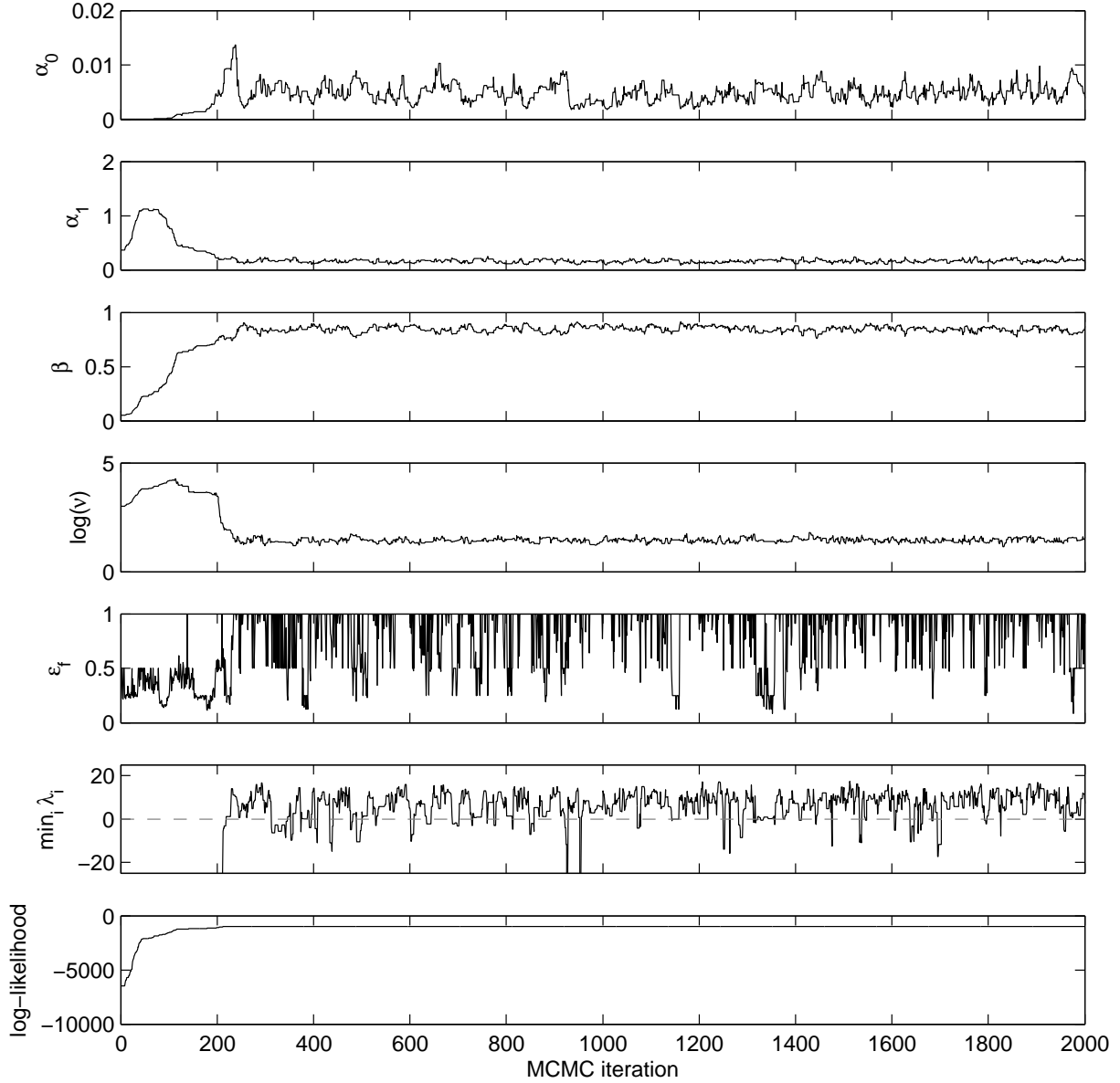


Figure 4: Diagnostics for a typical run of AMH-MALA with initial parameters set to the unrealistic values $\log(\alpha_0) = -10$, $\log(\alpha_1) = -1$, $\log(\beta) = -3$ and $\nu = 20$. The upper 4 panels are trace plots of parameters $\alpha_0, \alpha_1, \beta$ and $\log(\nu)$ where the logarithm is applied to latter for visual reasons. The 5. panel is a trace plot of the forward step size ε_f . The 6. panel depicts the smallest eigenvalue of $-H(\mathbf{x}_t)$, with smallest eigenvalue for the first 211 iterations being smaller than -25. The last panel shows the log-target target density at the current iteration, i.e. $\log \tilde{\pi}(\mathbf{x}_t)$.

log-transformed parameters $\alpha'_0 = \log(\alpha_0)$, $\alpha'_1 = \log(\alpha_1)$, $\beta' = \log(\beta)$ and $\nu' = \log(\nu - 2)$ to remove potential numerical problems related to the truncations imposed by the priors.

Table 1 provides mean CPU times, mean ESSes and mean minimum ESS per computing time for the parameters of the GARCH model (9-10) across 10 independent repeated runs of 5000 samples each. For **bayesGARCH** I used 5000 burn in iterations, whereas the remaining methods used 1000 burn in iterations. The reported CPU times excludes burn in. It should be noted that the Gibbs sampler in the **bayesGARCH** package is written partially in C and the computing times are therefore not directly comparable to the remaining methods, which are implemented fully in Matlab. It is seen that AMH-MALA produces the most effective samples per unit computing time for the methods written in Matlab, and also produces substantially better ESSes per iteration than the **bayesGARCH**. AMH-MALA and AMH-MALA(eig) produces similar results, indicating that there is little added value to using full spectral decomposition over the modified Cholesky factorization for this situation.

Figure 4 depicts various diagnostic output for a typical run of AMH-MALA applied to the parameters of (9-10). The initial parameters are set to highly ill informed values to illustrate the different behavior of AMH-MALA in transient and stationary regimes. It is seen that AMH-MALA takes shorter forward steps in the transient regime up to approximately iteration 220. The negative Hessian is severely indefinite for these iterations. This shows that choosing step size based on the energy error enables to AMH-MALA to make progress in the transient regime with the same tuning parameters as are used in the stationary regime. To contrast this, fixing $\varepsilon_f = \varepsilon_b = 1$ but otherwise keeping the setup identical to that reported in Figure 4 results in a single accepted move in the course of the 2000 iterations, indicating the need for different tuning parameters in stationary and transient regimes (Christensen et al., 2005).

Visual inspection of Figure 4 indicates that small values of ε_f are often associated with near zero minimum eigenvalues. This can be statistically confirmed as the correlation between $\log |\min_i \lambda_i|$ and ε_f is 0.63 for iterations 220-2000. This indicates that the adaptive step size procedure on average sees both large positive- and large negative curvature information as useful and consequently takes long step sizes, whereas it takes shorter step sizes when very little curvature information is available in some direction. Still there is a small positive correlation of 0.24 between $\min_i \lambda_i$ and the acceptance probability, indicating that AMH-MALA performs slightly better in regions of the support where the target is log-concave.

3.2 Bayesian binary response regression

This section considers Bayesian inference for two types of binary response generalized linear models. The models are included in order to compare the proposed methodology with that of Girolami and Calderhead

| Model | Method | CPU time (s) | minimum ESS | median ESS | maximum ESS | minimum ESS per second |
|--|-----------------|-----------------|----------------|---------------|----------------|---------------------------|
| Australian credit data set ($d = 15, n = 690$) | | | | | | |
| logit | AMH-MALA | 2.6 | 436 | 579 | 725 | 167 |
| logit | sMMALA | 1.6 | 436 | 591 | 745 | 271 |
| probit | AMH-MALA | 3.4 | 575 | 774 | 919 | 167 |
| probit | sMMALA | 1.8 | 491 | 665 | 869 | 280 |
| probit | Adaptive sMMALA | 3.3 | 475 | 652 | 809 | 142 |
| German credit data set ($d = 25, n = 1000$) | | | | | | |
| logit | AMH-MALA | 3.6 | 417 | 570 | 707 | 117 |
| logit | sMMALA | 2.1 | 432 | 616 | 751 | 202 |
| probit | AMH-MALA | 4.5 | 579 | 747 | 886 | 129 |
| probit | sMMALA | 2.4 | 534 | 700 | 846 | 226 |
| probit | Adaptive sMMALA | 4.4 | 488 | 649 | 785 | 111 |
| Heart data set ($d = 14, n = 270$) | | | | | | |
| logit | AMH-MALA | 2.0 | 362 | 468 | 579 | 176 |
| logit | sMMALA | 1.3 | 364 | 473 | 587 | 273 |
| probit | AMH-MALA | 2.5 | 612 | 760 | 883 | 247 |
| probit | sMMALA | 1.4 | 451 | 593 | 734 | 331 |
| probit | Adaptive sMMALA | 2.4 | 475 | 590 | 719 | 197 |
| Pima Indian data set ($d = 8, n = 532$) | | | | | | |
| logit | AMH-MALA | 2.2 | 1043 | 1184 | 1296 | 479 |
| logit | sMMALA | 1.4 | 1010 | 1174 | 1314 | 732 |
| probit | AMH-MALA | 2.7 | 1143 | 1282 | 1428 | 425 |
| probit | sMMALA | 1.4 | 1089 | 1253 | 1480 | 752 |
| probit | Adaptive sMMALA | 2.6 | 1116 | 1242 | 1454 | 431 |
| Ripley data set ($d = 7, n = 250$) | | | | | | |
| logit | AMH-MALA | 1.3 | 285 | 375 | 467 | 227 |
| logit | sMMALA | 0.6 | 291 | 387 | 464 | 506 |
| probit | AMH-MALA | 1.8 | 387 | 536 | 623 | 212 |
| probit | sMMALA | 0.8 | 287 | 379 | 490 | 381 |
| probit | Adaptive sMMALA | 1.8 | 293 | 391 | 506 | 161 |

Table 2: Effective sample sizes and CPU times for the Bayesian binary response regressions. Best performances are indicated with bold font. “logit” correspond models with logistic link function. In this case the negative Hessian and Fisher information matrix coincides. “probit” correspond to the standard normal cumulative distribution function as the inverse link function. In this case the negative Hessian is different from the Fisher information matrix. sMMALA replicates the simplified manifold MALA of Girolami and Calderhead (2011) whereas Adaptive sMMALA uses the metric tensor of Girolami and Calderhead (2011) along with adaptive step size selection.

(2011). Specifically, I consider models for observed binary responses $\mathbf{y} = (y_1, \dots, y_n)$ on the form

$$\begin{aligned} P(y_i = 1) &= \rho[(X\beta)_i], \quad i = 1, \dots, n, \\ \beta &\sim N(0, 100I_d). \end{aligned} \tag{11}$$

Here $X \in \mathbb{R}^{n \times d}$ is a design matrix and the inverse link function ρ is specified either as a logit link corresponding to $\rho(x) = \exp(x)/(1 + \exp(x))$ or the probit link corresponding to $\rho(x) = \Phi(x)$ where Φ denotes the $N(0, 1)$ distribution function. For both link functions, the Fisher information matrix is available in closed form, and for the logit link the negative Hessian of log-likelihood function associated with (11) coincides with the Fisher information matrix, whereas this is not the case for the probit model. However, the negative Hessian is still positive definite in the relevant region for the probit model.

I consider the collection of 5 data sets used by Girolami and Calderhead (2011) where n ranges between 250 and 1000 and d ranges between 7 and 25. The sMMALA method using G_{GC} is used as a reference. For the logit model, this amounts to a replication of the simplified MMALA-part of the Monte Carlo experiment of Girolami and Calderhead (2011), and therefore admits calibration of their results against those presented here. In particular, I recoded the method of Girolami and Calderhead (2011) so that all codes use the same routines for evaluating likelihoods, gradients and Hessians to make the comparison as fair as possible. For AMH-MALA I employed $\gamma = 2.0$ and Algorithm 1 with $\beta = 20.0$, $\rho = 0.7$. In this setting, Algorithm 1 works mainly as a safeguard against numerical problems occurring when some $\rho[(X\beta)_i] \rightarrow 0$ or $\rho[(X\beta)_i] \rightarrow 1$. The results are presented in Table 2. Through out, I collect 5000 samples after 5000 iterations of burn in, and the timings are for producing the post burn in samples. All experiments are repeated 10 times and reported numbers are averages across these replica. In Girolami and Calderhead (2011), the simplified MMALA was found to be the best method for the logit model for 4 out 5 data sets when other contenders included the Riemann manifold HMC and full manifold MALA and the performance measure was the minimum (over β) ESS produced per unit of time.

For the logit model, AMH-MALA may be interpreted as an adaptive step size version of Girolami and Calderhead (2011)'s simplified MMALA, I see that the line search mechanism leads to approximately a factor 2 increase computing time, whereas the number of effective samples produced per iteration are approximately the same. Looking at the results reported in Table 3-7 in Girolami and Calderhead (2011) using simplified MMALA as a reference, I find that AMH-MALA performance roughly on par with Riemann manifold HMC for this model and these data sets.

For the probit model, where $-H(\beta)$ and G_{GC} do not coincide, I see slightly larger differences in terms of effective sample size in favor of AMH-MALA, whereas the relative consumption of CPU time is roughly the

same as in the logit case. To further investigate this find, I also implemented a method based on G_{GC} but otherwise identical to AMH-MALA and denote this method Adaptive sMMALA. It is seen that the improved ESSes appear to be a feature of the application of the Hessian rather than adaptive step size selection as the ESSes of sMMALA and Adaptive sMMALA are roughly the same. From this I may conclude that the negative Hessian may be a better alternative than the Fisher information-based metric tensor for models where the Hessian is positive definite in all relevant regions.

4 Discussion

This paper makes usage of the Gill et al. (1981) modified Cholesky factorizations for producing positive definite metric tensors from the Hessian matrix for simplified manifold MALA methods. A new adaptive step size procedure that resolves the shortcomings of metric tensors derived from the Hessian in regions where the log-target has near zero curvature in some direction is proposed. The adaptive step size selection also appears to alleviate the need for different tuning parameters in transient and stationary regimes. The combination of the two constitute a large step towards developing reliable manifold MCMC methods that can be implemented for models with unknown or intractable Fisher information, and even for targets that does not admit a factorization into prior and likelihood. Through examples of low to moderate dimension, it is shown that proposed methodology performs very well relative to alternative MCMC methods.

To handle high-dimensional problems, it is likely that a HMC variant of the proposed methodology is needed. One avenue would be to make $G(\mathbf{x})$ a smooth function via the usage of soft-max functions (Betancourt, 2013) in Algorithm 2 and implement full Riemann manifold HMC along the lines of Girolami and Calderhead (2011). This approach would enable the exploitation of sparsity of the Hessian not afforded by methods based on spectral decompositions (Betancourt, 2013), but would still require computing third derivatives of $\log \tilde{\pi}$. An interesting alternative that is currently being investigated involves embedding HMC into a population MCMC framework where each member of the population has the same target. In such a setup, one member of the population is expended in each MCMC iteration for calculating a position-specific mass matrix and time integration step size using the modified Cholesky factorization and adaptive step size selection procedure proposed here. These parameters are then applied in standard HMC updates of the remaining population members to mimic the effects of Riemann manifold HMC while retaining a computationally attractive separable Hamiltonian.

Another avenue for further work is to extend the adaptive step size methodology via energy error arguments of Section 2.3 to other MCMC methods, via the observation that other, possibly non-symplectic, numerical integration schemes applied to Hamilton’s equations associated with (7) leads to different known

proposal distributions. In particular, a symplectic Euler type B integrator (Leimkuhler and Reich, 2004, page 26) lead to a $N(\mathbf{x} + \varepsilon^2 G(\mathbf{x})^{-1} g(\mathbf{x}), \varepsilon^2 G(\mathbf{x})^{-1})$ proposal which nests (for $\varepsilon = 1$) the stochastic Newton MCMC method of Martin et al. (2012). A standard Euler integrator lead to a position specific scale random walk proposal $N(\mathbf{x}, \varepsilon^2 G(\mathbf{x})^{-1})$.

References

- Andrieu, C., A. Doucet, and R. Holenstein (2010). Particle Markov chain Monte Carlo methods. *Journal of the Royal Statistical Society: Series B (Statistical Methodology)* 72(3), 269–342.
- Ardia, D. and L. F. Hoogerheide (2010, dec). Bayesian Estimation of the GARCH(1,1) Model with Student-t Innovations . *The R Journal* 2(2), 41–47.
- Beskos, A., N. Pillai, G. Roberts, J.-M. Sanz-Serna, and A. Stuart (2013). Optimal tuning of the hybrid Monte Carlo algorithm. *Bernoulli* 19(5A), 1501–1534.
- Betancourt, M. (2013). A general metric for Riemannian manifold Hamiltonian Monte Carlo. In F. Nielsen and F. Barbaresco (Eds.), *Geometric Science of Information*, Volume 8085 of *Lecture Notes in Computer Science*, pp. 327–334. Springer Berlin Heidelberg.
- Betancourt, M. J., S. Byrne, and M. Girolami (2014). Optimizing the integrator step size for hamiltonian monte carlo. arXiv:1411.6669.
- Brooks, S., A. Gelman, G. Jones, and X.-L. Meng (Eds.) (2011). *Handbook of Markov Chain Monte Carlo*. Chapman & Hall/CRC Handbooks of Modern Statistical Methods. Chapman & Hall/CRC.
- Christensen, O. F., G. O. Roberts, and J. S. Rosenthal (2005). Scaling limits for the transient phase of local Metropolis-Hastings algorithms. *Journal of the Royal Statistical Society: Series B (Statistical Methodology)* 67(2), 253–268.
- Davis, T. A. (2006). *Direct Methods for Sparse Linear Systems*, Volume 2 of *Fundamentals of Algorithms*. SIAM.
- Duane, S., A. Kennedy, B. J. Pendleton, and D. Roweth (1987). Hybrid Monte Carlo. *Physics Letters B* 195(2), 216 – 222.
- Gelman, A., J. B. Carlin, H. S. Stern, D. B. Dunson, A. Vehtari, and D. Rubin (2014). *Bayesian Data Analysis* (3 ed.). CRC Press.

- Gelman, A., G. Roberts, and W. Gilks (1996). Efficient Metropolis jumping rules. In J. M. Bernardo et al. (Eds.), *Bayesian Statistics*, Volume 5, pp. 599. OUP.
- Geyer, C. J. (1992). Practical Markov chain Monte Carlo. *Statistical Science* 7(4), pp. 473–483.
- Gilks, W. R., G. O. Roberts, and E. I. George (1994). Adaptive direction sampling. *Journal of the Royal Statistical Society. Series D (The Statistician)* 43(1), pp. 179–189.
- Gill, P. and W. Murray (1974). Newton-type methods for unconstrained and linearly constrained optimization. *Mathematical Programming* 7, 311–350.
- Gill, P. E., W. Murray, and M. H. Wright (1981). *Practical Optimization*. London: Academic Press.
- Girolami, M. and B. Calderhead (2011). Riemann manifold Langevin and Hamiltonian Monte Carlo methods. *Journal of the Royal Statistical Society: Series B (Statistical Methodology)* 73(2), 123–214.
- Griewank, A. (2000). *Evaluating Derivatives: Principles and Techniques of Algorithmic Differentiation*. SIAM, Philadelphia.
- Guerrera, T., H. Rue, and D. Simpson (2011). Discussion of "Riemann manifold Langevin and Hamiltonian Monte Carlo" by Girolami and Calderhead. *Journal of the Royal Statistical Society: Series B (Statistical Methodology)* 73(2), 123–214.
- Hastings, W. (1970). Monte Carlo sampling methods using Markov chains and their applications. *Biometrika* 57, 97–109.
- Hoffman, M. D. and A. Gelman (2014). The no-u-turn sampler: Adaptively setting path lengths in Hamiltonian Monte Carlo. *Journal of Machine Learning Research* 15, 1593–1623.
- Jasra, A. and S. Singh (2011). Discussion of "Riemann manifold Langevin and Hamiltonian Monte Carlo" by Girolami and Calderhead. *Journal of the Royal Statistical Society: Series B (Statistical Methodology)* 73(2), 123–214.
- Leimkuhler, B. and S. Reich (2004). *Simulating Hamiltonian dynamics*. Cambridge University Press.
- Liu, J. S. (2001). *Monte Carlo strategies in scientific computing*. Springer series in statistics. springer.
- Livingstone, S. and M. Girolami (2014). Information-geometric Markov chain Monte Carlo methods using diffusions. *Entropy* 16(6), 3074–3102.

- Martin, J., L. Wilcox, C. Burstedde, and O. Ghattas (2012). A stochastic Newton MCMC method for large-scale statistical inverse problems with application to seismic inversion. *SIAM Journal on Scientific Computing* 34(3), A1460–A1487.
- McNeil, A. J., R. Frey, and P. Embrechts (2005). *Quantitative Risk Management: Concepts, Techniques, and Tools*. Princeton series in Finance. Princeton University Press.
- Metropolis, N., A. W. Rosenbluth, M. N. Rosenbluth, A. H. Teller, and E. Teller (1953). Equation of state calculations by fast computing machines. *Journal of Chemical Physics* 21, 1087–1092.
- Neal, R. M. (2010). MCMC using Hamiltonian dynamics. In *Handbook of Markov Chain Monte Carlo*, pp. 113–162.
- Nocedal, J. and S. J. Wright (1999). *Numerical Optimization*. Springer.
- Robert, C. P. and G. Casella (2004). *Monte Carlo Statistical Methods* (second ed.). Springer.
- Roberts, G. and O. Stramer (2002). Langevin diffusions and Metropolis-Hastings algorithms. *Methodology And Computing In Applied Probability* 4(4), 337–357.
- Roberts, G. O. and J. S. Rosenthal (2001). Optimal scaling for various Metropolis-Hastings algorithms. *Statistical Science* 16(4), 351–367.
- Roberts, G. O. and R. L. Tweedie (1996). Exponential convergence of Langevin distributions and their discrete approximations. *Bernoulli* 2(4), 341–363.
- Sanz-Serna, J. M. (2011). Discussion of "Riemann manifold Langevin and Hamiltonian Monte Carlo" by Girolami and Calderhead. *Journal of the Royal Statistical Society: Series B (Statistical Methodology)* 73(2), 123–214.
- Schnabel, R. and E. Eskow (1990). A new modified Cholesky factorization. *SIAM Journal on Scientific and Statistical Computing* 11(6), 1136–1158.
- Schnabel, R. and E. Eskow (1999). A revised modified Cholesky factorization algorithm. *SIAM Journal on Optimization* 9(4), 1135–1148.
- Xifara, T., C. Sherlock, S. Livingstone, S. Byrne, and M. Girolami (2014). Langevin diffusions and the Metropolis-adjusted Langevin algorithm. *Statistics & Probability Letters* 91(0), 14 – 19.
- Zhang, Y. and C. Sutton (2011). Quasi-Newton Markov chain Monte Carlo. In *Advances in Neural Information Processing Systems (NIPS)*.

Algorithm 2 A variant of the modified Cholesky decomposition of Gill et al. (1981).

Input: $d \times d$ symmetric matrix A and a small scale factor u .

step 0,1: $\tilde{L} \leftarrow I_d$.

step 0,2: $D_{j,j} \leftarrow A_{j,j}$, $j = 1, \dots, d$.

step 0,3: $\nu \leftarrow \max_j |A_{j,j}|$.

step 0,4: $\xi \leftarrow \max_{i < j} |A_{i,j}|$.

step 0,5: $\phi^2 \leftarrow \max(\nu, \xi/\sqrt{d^2 - 1}, u)$.

step 0,6: $\delta \leftarrow u \max(\nu, \xi, 1)$.

for $j = 1$ to n

step 1: **if** ($j > 1$) $\tilde{L}_{j,k} \leftarrow \tilde{L}_{j,k}/D_{k,k}$, $k = 1, \dots, j-1$.

step 2: **if** ($j < d$) $\tilde{L}_{j+1:d,j} \leftarrow A_{j+1:d,j}$.

step 3: **if** ($1 < j < d$) $\tilde{L}_{j+1:d,j} \leftarrow \tilde{L}_{j+1:d,j} - (\tilde{L}_{j+1:d,1:j-1})(\tilde{L}_{j,1:j-1})^T$.

step 4: **if** ($j < d$) $\theta_j \leftarrow \max_{k < j} |\tilde{L}_{k,j}|$ **else** $\theta_j \leftarrow 0$.

step 5: $D_{j,j} \leftarrow \max(\delta, |\tilde{L}_{j,j}|, \theta_j^2/\phi^2)$.

step 6: **if** ($j < d$) $D_{k,k} \leftarrow D_{k,k} - (\tilde{L}_{k,j})^2/D_{j,j}$, $k = j+1, \dots, d$.

end for

Return \tilde{L} and D (so that $\tilde{L}D\tilde{L}^T = A + J$) or $L = \tilde{L}D^{1/2}$ (so that $LL^T = A + J$).

A A version of the Gill et al. (1981) modified Cholesky

This section recaptures GMW's square root-free modified Cholesky algorithm for finding lower triangular matrix \tilde{L} with $\tilde{L}_{i,i} = 1$, $i = 1, \dots, d$ and diagonal matrix D so that

$$\tilde{L}D\tilde{L}^T = A + J.$$

The conventional lower triangular Cholesky factor given in (3) obtains as $L = \tilde{L}D^{1/2}$. GMW's approach takes as vantage points:

1. A uniform lower bound on the diagonal elements of D (or L), i.e. $D_{j,j} = L_{j,j}^2 \geq \delta$, $j = 1, \dots, d$ for a small positive constant δ .
2. A uniform upper bound on the absolute off-diagonal elements of $L = \tilde{L}D^{1/2}$ that ensures that \hat{A} is positive definite and numerically stable, i.e. $|\tilde{L}_{i,j}\sqrt{D_{j,j}}| \leq \phi$, $i = 2, \dots, d$, $j < i$.

By taking $\phi^2 = \max(\nu, \xi/\sqrt{d^2 - 1}, u)$ where ν and ξ are the maximal absolute diagonal- and off-diagonal elements respectively, Gill et al. (1981) show that \hat{A} is positive definite while at the same time a bound on the infinity norm of J is minimized. Throughout this paper, δ is taken to be $u \max(\nu, \xi, 1)$. The scale factor u is commonly taken to be close to machine accuracy for optimization applications, but in this work it is left as tuning parameter.

GMW's approach for implementing the above bounds is based on a square root free Cholesky factorization (Nocedal and Wright, 1999, p. 146) and is given in Algorithm 2. Gill et al. (1981) observed that immediately

after step 3 in the j th iteration of the algorithm, the j th column of the unfinished \tilde{L} contains $D_{j,j}$ times the j th column of the final \tilde{L} . Therefore $D_{j,j}$ can be chosen (step 4 and 5) during the course of the algorithm to respect the two bounds given above. The difference in $D_{j,j}$ between after and before step 4 in iteration j amounts to the j th diagonal element of J , and simply removing steps 4 and 5 corresponds to a standard square root free Cholesky algorithm. The modifications essentially adds $O(d^2)$ comparisons to the computational complexity relative to the standard dense Cholesky algorithm it derives from, and is therefore asymptotically insignificant comparing to the $O(d^3/6)$ floating point operations needed to carry out the latter.

B Proof of Proposition 1

Irreducibility of the update of \mathbf{x} in steps 1-4 is ensured by the fact that the proposal distribution is Gaussian with finite and positive definite covariance matrix whenever $0 < \varepsilon(\mathbf{x}, \mathbf{w}) < \infty$ for all (\mathbf{x}, \mathbf{w}) in the support of $\pi(\mathbf{x}, \mathbf{w})$. The update of \mathbf{w} in step 5 is trivially irreducible since it amounts to iid sampling. Consequently the overall update in steps 1-5 is irreducible as any point on the support of the target is attainable in each iteration.

Aperiodicity of the update of \mathbf{x} is ensured by the fact that it involves a non-trivial accept-reject in step 4 (Robert and Casella, 2004, section 7.3.2) and aperiodicity of the update of \mathbf{w} is trivial since it is iid. Consequently, the overall update in steps 1-5 is thus aperiodic.

To verify that $\pi(\mathbf{x}, \mathbf{w})$ is the invariant distribution of steps 1-5, first observe that for each given \mathbf{w}_t , steps 1-4 define a reversible MH step with $\pi(\mathbf{x})$ as invariant distribution. The reversibility is consequence of the fact that $\varepsilon_f, \varepsilon_b$ are computed with the same \mathbf{w} -argument, and therefore within steps 1-4 of each iteration $\varepsilon(\mathbf{x}, \mathbf{w})$ is effectively a function of the first argument only. Denote by $A(\mathbf{x}_{t+1}|\mathbf{x}_t, \mathbf{w}_t)$ the transition kernel associated with steps 1-4. Then the overall transition kernel of steps 1-5 may be written as $B(\mathbf{x}_{t+1}, \mathbf{w}_{t+1}|\mathbf{x}_t, \mathbf{w}_t) = A(\mathbf{x}_{t+1}|\mathbf{x}_t, \mathbf{w}_t)\pi(\mathbf{w}_{t+1})$. That $\pi(\mathbf{x}, \mathbf{w})$ is the invariant distribution of B is then seen via

$$\begin{aligned} \int \int \pi(\mathbf{x}, \mathbf{w}) B(\mathbf{x}', \mathbf{w}'|\mathbf{x}, \mathbf{w}) d\mathbf{x} d\mathbf{w} &= \pi(\mathbf{w}') \int \pi(\mathbf{w}) \int A(\mathbf{x}'|\mathbf{x}, \mathbf{w}) \pi(\mathbf{x}) d\mathbf{x} d\mathbf{w}, \\ &= \pi(\mathbf{w}') \pi(\mathbf{x}') = \pi(\mathbf{x}', \mathbf{w}'), \end{aligned}$$

where the second equality follows from the reversibility of steps 1-4 for each \mathbf{w} .